Nanoclay Suspension-Enabled Extrusion Bioprinting of 3D Soft Structures

Yifei Jin[1,*], Ruitong Xiong[2], Patrick J. Antonelli[3], Christopher J. Long[4], Christopher W. McAleer[4], James J. Hickman[4], Yong Huang [2,**]

[1] Mechanical Engineering Department, University of Nevada Reno, Reno, NV 89557, USA

[2] Department of Mechanical and Aerospace Engineering, University of Florida, Gainesville, FL 32611, USA

[3] Department of Otolaryngology, University of Florida, Gainesville, FL 32611, USA

[4] NanoScience Technology Center, University of Central Florida, Orlando, FL 32816, USA

* Corresponding author, MS0312, University of Nevada Reno, Reno, NV 89557, USA

Phone: 001-775-784-1412, Fax: 001-775-784-1390, Email: yifeij@unr.edu

** Corresponding author, P. O. Box 116250, University of Florida, Gainesville, FL 32611, USA,

Phone: 001-352-392-5520, Fax: 001-352-392-7303, Email: yongh@ufl.edu

ABSTRACT

Three-dimensional (3D) extrusion printing of cellular/acellular structures with biocompatible materials has been widely investigated in recent years. However, the requirement of suitable solidification rate of printable ink materials constrains the utilization of extrusion-based 3D printing technique. In this study, the nanoclay yield-stress suspension-enabled extrusion-based 3D printing system has been investigated and demonstrated to overcome solidification rate constraints during printing. Utilizing the liquid-solid transition property of nanoclay suspension, two

fabrication approaches, including nanoclay support bath-enabled printing and nanoclay-enabled direct printing, have been proposed. For the former approach, nanoclay (Laponite EP) has been used as a support bath material to fabricate alginate-based tympanic membrane patches. The constituents of alginate-based ink have been investigated to have the desired mechanical property of alginate-based tympanic membrane patches and facilitate the printing process. For the latter approach, nanoclay (Laponite XLG) has been used as an internal scaffold material to help print poly (ethylene glycol) diacrylate (PEGDA)-based neural chambers, which can be further cross-linked in air. Mechanical stress analysis has been performed to explore the geometric limitation of printable Laponite XLG-PEGDA neural chambers.

Keywords: 3D printing, nanoclay suspension, yield-stress material, tympanic membrane patch, neural chamber

1. INTRODUCTION

Three-dimensional (3D) bioprinting techniques enable the freeform fabrication of complex cellular and/or acellular structures from various liquid ink materials and provide an effective way to on-demand fabricate products for diverse bio-applications [1-3]. Among different bioprinting techniques [4-8], micro-extrusion has been widely used due to its easy implementation, wide range of printable materials, and relatively high printing efficiency. Using cell-laden and/or acellular inks, complex 3D structures have been successfully printed using micro-extrusion, which can be used either as scaffold-free cellular constructs [5, 7-9] or scaffold structures for cell seeding [10-12].

In micro-extrusion, applied ink materials must have a suitable cross-linking rate to facilitate a continuous 3D printing process, which limits the selection of various ink materials. If the ink cross-linking rate is too fast after printing, the extrusion nozzle can be easily clogged due to the short standoff distance. For instance, when printing sodium alginate in a cross-linking agent bath such as calcium chloride, surface tension can bring calcium ions into the dispensing nozzle, the fast cross-linking process in the nozzle may lead to the nozzle clogging [7]. In contrast, if the cross-linking rate is too slow, it usually takes a long time to solidify a deposited layer before printing a next layer. For instance, when printing poly (ethylene glycol) diacrylate (PEGDA), the cross-linking process may take a few minutes under ultraviolet (UV) radiation [13]. Thus, the next PEGDA layer can't be printed atop the previous layer until it is UV cross-linked for a few minutes, which decreases the fabrication efficiency significantly. As a result, it is necessary to develop new 3D printing strategies that are suitable to 3D extrusion print liquid build materials demanding a fast and/or slow cross-linking rate.

In this study, biomedical applications of a nanoclay suspension-enabled extrusion-based 3D printing system have been demonstrated in fabricating soft structures from various hydrogels and/or hydrogel composites. Since nanoclay suspension has a unique yield-stress property, it can easily transit between liquid and solid states upon differently stressed conditions. When the applied stress is higher than the yield stress of a nanoclay suspension, it behaves liquid like; otherwise, it behaves solid like. Nanoclay Laponite has been mixed with various hydrogel precursors to prepare nanocomposite hydrogels with desirable mechanical and rheological properties for various biomedical applications. For example, Chang et al. have mixed nanoclay Laponite with poly (ethylene glycol) for bone tissue engineering applications [14], Ghadiri et al. have prepared

nanoclay Laponite/alginate composites for cartilage and/or bone tissue regeneration [15], and Gaharwar et al. have added nanoclay Laponite to gelatin solution to prepare a hemostatic agent [16]. However, none of aforementioned studies have used nanoclay Laponite to facilitate the extrusion 3D printing process. Herein, two nanoclay suspension-based printing strategies have been developed: using nanoclay suspension as a yield-stress support bath, alginate-based tympanic membranes have been printed and gradually cross-linked in the bath. During cross-linking, the nanoclay support bath can help hold the ungelled alginate structures *in situ* stably; using nanoclay suspension as a yield-stress internal scaffold material, Laponite-PEGDA precursor nanocomposite-based neural chambers have been directly printed in air and cross-linked thereafter.

In the following sections, the nanoclay suspension-enabled extrusion printing system is introduced in Section 2. Then the printing of alginate-based tympanic membrane patch and PEGDA-based neural chamber is discussed in Sections 3 and 4, respectively. Some discussions on the proposed printing system are offered in Section 5. Finally, some conclusions and future work are summarized in Section 6.

2. NANOCLAY SUSPENSION-ENABLED EXTRUSION PRINTING SYSTEM

Laponite nanoclay is one type of smectite minerals, which is composed of crystalline nanosilicates with a diameter of approximately 25 nm and a thickness of 1 nm and the most commonly used nanoclay minerals in bio-related applications. When dispersed in water, sodium ions dissociate from the surface of the nanosilicates, leaving the faces of each disc negatively charged. Meanwhile, hydroxide ions dissociate from the edges, resulting in positive charges on the edges as shown in Fig. 1(a). Thus, the charge distribution makes Laponite nanosilicates form a stable 3D arrangement,

which is presumably considered as “house-of-cards” when the aqueous Laponite suspension equilibrates as shown in Fig. 1(b). This unique “house-of-cards” arrangement enables the Laponite suspension to have yield stress, which is a result of the threshold energy required to disrupt the “house-of-cards” arrangement before the suspension can flow. In this study, two types of Laponite suspensions are utilized for extrusion printing applications: Laponite EP and Laponite XLG. For the former, organic modification has been performed on Laponite EP nanosilicates and it is not reactive with ionic solutions. For the latter, the nanosilicates have high purity and a certified low heavy-metal content.

The rheological properties including the yield stress and shear moduli of the Laponite EP and Laponite XLG suspensions were investigated and measured elsewhere [9, 12]. It is found that at extremely low shear rates both Laponite EP and Laponite XLG suspensions present stress and their yield stress values can be calculated as approximately 8.8 Pa [9] and 217.5 Pa [12], respectively, using a classic Herschel-Buckley model. In addition, the frequency sweeps show that two nanoclay suspensions have the storage modulus higher than the loss modulus, indicating that both Laponite EP and Laponite XLG suspensions show solid-like behavior under low strain conditions.

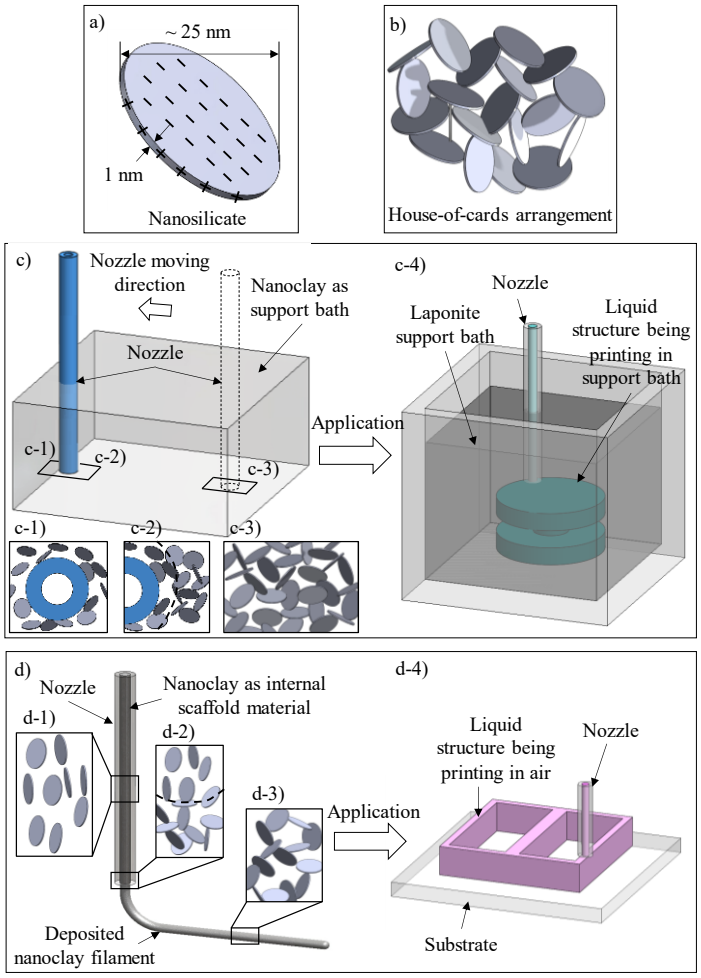

FIGURE 1: Nanoclay and nanoclay suspension-enabled extrusion-based 3D printing system. Schematics of (a) nanosilicate and (b) "house-of-cards" arrangement. (c) Mechanism of nanoclay support bath-enabled printing strategy. (d) Mechanism of nanoclay-enabled direct printing in air strategy.

Due to its unique yield-stress rheological property, Laponite suspension is a solid-like liquid, which can readily transit between liquid and solid states upon differently stressed conditions. This liquid/solid transition capability enables Laponite suspensions to be used either as a support bath material (Laponite EP) (from solid to liquid transition) or as an internal scaffold material (Laponite

XLG) (from liquid to solid transition) for 3D printing applications. As a result, the nanoclay suspension-enabled extrusion-based 3D printing system has been proposed and investigated as reported in some studies [9, 12]. Herein, the feasibility of the nanoclay suspension-enabled 3D printing system is further demonstrated during printing of complex soft structures from different biocompatible ink materials, which proves the effectiveness of the proposed 3D printing system for biomedical applications.

2.1 Nanoclay Support Bath-Enabled Printing Approach

Since Laponite EP is insensitive to ionic changes, it is mixable with some ionic cross-linking agents such as calcium chloride ($CaCl_2$) solutions while retaining its original yield-stress property. Thus, the mixture can be used as a support bath to print ionic cross-linking materials such as sodium alginate. The mechanism of this fabrication approach is illustrated in Fig. 1(c). When a dispensing nozzle moves in a Laponite EP bath, nanosilicates at the nozzle tip may undergo the shear stress higher than the yield stress, and the "house-of-cards" arrangement of these affected nanosilicates is physically disturbed. As such, the localized Laponite EP suspension behaves like liquid as shown in Fig. 1(c-1). Once the nozzle travels through, the applied shear stress disappears and the disturbed nanosilicates recover the "house-of-cards" arrangement rapidly as shown in Fig. 1(c-2). Thus, the crevasse behind the translating nozzle can be filled by the liquid-like nanoclay suspension, and the deposited liquid structure is trapped and supported in the nanoclay bath. The Laponite EP suspension away from the nozzle doesn't experience any shear stress, and the "house-of-cards" arrangement is maintained as shown in Fig. 1(c-3). As a result, the Laponite EP suspension behaves solid like to hold the printed structure stably *in situ* even for a long time. For demonstration herein, Laponite EP-$CaCl_2$ is selected as the support bath material to print alginate-

based structures *in situ* and gradually cross-link printed structures in the bath as shown in Fig. 1(c-4).

2.2 Nanoclay-Enabled Direct Printing Approach

Due to the relatively higher yield stress of Laponite XLG suspension, it is selected as the internal scaffold material to facilitate the direct printing of liquid hydrogel (for example, PEGDA)-based structures in air. Herein, the liquid-to-solid transition of Laponite XLG suspensions from the sheared condition to non-sheared condition is utilized and the nanoclay-enabled direct printing in air strategy is proposed. The mechanism of this fabrication approach is illustrated in Fig. 1(d). When the applied pressure is higher than the yield stress of the Laponite XLG suspension in the nozzle during extrusion, the "house-of-cards" arrangement is disrupted, and the solid-like Laponite XLG nanoclay suspension liquefies to be readily extruded out of the nozzle as shown in Fig. 1(d-1). At the exist of the nozzle tip, the disrupted nanosilicates rapidly recover the "house-of-cards" arrangement as shown in Fig. 1(d-2) when the shear stress diminishes. When the Laponite XLG suspension is deposited atop a substrate or a previously printed layer, the disordered nanoclay suspension reverts to a solid-like state with a yield stress as it recovers the "house-of-cards" arrangement as shown in Fig. 1(d-3). Due to its yield stress, the deposited Laponite XLG-based feature has the self-supporting property and can maintain its shape stably in air without needing any additional cross-linking process. Since Laponite XLG can be mixed with different hydrogel precursors such as PEGDA and each resultant nanocomposite hydrogel inherits the similar yield-stress and self-supporting property of Laponite XLG [12], such nanocomposite hydrogels can be printed directly in air. For demonstration, Laponite XLG-PEGDA is used as the ink material to

print neural chambers using this nanoclay-enabled direct printing approach as shown in Fig. 1(d-4).

3. PRINTING OF ALGINATE-BASED TYMPANIC MEMBRANE PATCHES IN NANOCLAY SUPPORT BATH

3.1 Introduction of Tympanic Membrane and Tympanic Membrane Patch

The tympanic membrane is a multi-layered structure which captures and transmits sound from the environment through the ossicular chain of the middle ear to the inner ear, as shown in Fig. 2(a) and (b). Damage to the tympanic membrane, from otitis media or trauma (as shown in Fig. 2(c)), typically results in the hearing loss [17]. Thus, it is necessary to on-demand fabricate artificial tympanic membrane patches to facilitate repair of tympanic membranes.

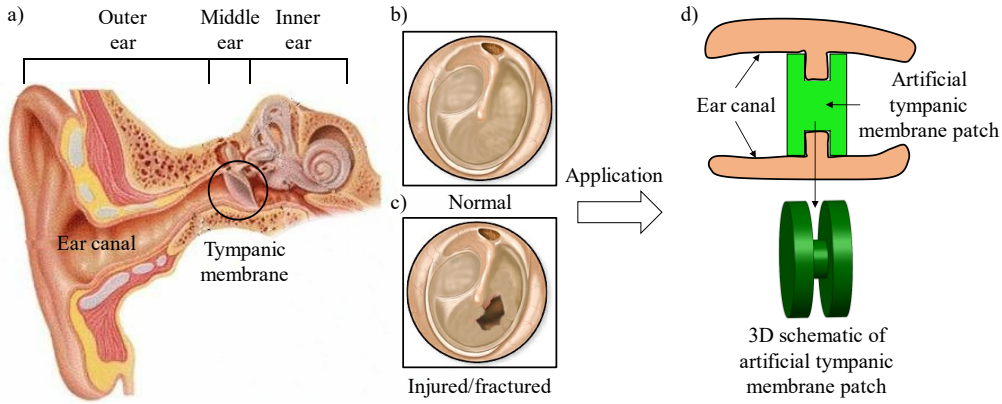

FIGURE 2: (a) Ear anatomy, (b) normal and (c) injured/fractured tympanic membrane, and (d) artificial tympanic membrane patch with three-layered structure.

Recent advances in 3D printing provide a powerful tool to design and fabricate biomimetic tympanic membrane grafts, which can reproduce specific structural features of human tympanic

membrane [18]. Alginate, a natural polysaccharide, has been widely used in tissue engineering to fabricate artificial organs/tissues due to its versatile functionality, mild cross-linking conditions, low cost, biocompatibility, low toxicity, and environmentally friendly nature [19]. It is also one of the most commonly used biomaterials for tympanic membrane repair and regeneration [20-22]. As such, alginate-based tympanic membrane patches with a three-layered morphology are 3D printed using the nanoclay support bath-enabled printing for tympanic membrane repair as shown in Fig. 2(d).

3.2 Materials and Methods

3.2.1 Material preparation for alginate-based tympanic membrane patch printing

Firstly, 8.0% (w/v) Laponite EP (BYK Additives Inc., Gonzales, Texas) suspension (pH ≈ 7.0) was prepared by dispersing the appropriate amount of dry Laponite EP powders in deionized (DI) water at room temperature. An overhead stirrer (Thermo Fisher Scientific, Waltham, MA) was used to continuously mix the Laponite suspension at 500 rpm for 90 minutes. The resulted Laponite suspension was stored in sealed containers and aged for at least one day. Secondly, 4.0% (w/v) calcium chloride ($CaCl_2$, Sigma-Aldrich, St. Louis, MO) solution was used as the cross-linking agent of sodium alginate and prepared by dispersing and dissolving the appropriate amount of dry $CaCl_2$ powder in deionized (DI) water at room temperature. By mixing stock 8.0% (w/v) Laponite EP suspension 1:1 (v:v) with 4.0% (w/v) $CaCl_2$ solution using an overhead stirrer at room temperature, a 4.0% (w/v) Laponite EP suspension with 2.0% (w/v) $CaCl_2$ was prepared and used as the support bath for alginate-based tympanic membrane patch printing, which has the similar rheological properties with Laponite EP as reported [9]. The mixed Laponite EP-$CaCl_2$ suspension was stored in a sealed container and aged for at least one day. Before each use, a centrifuge (5804R,

Eppendorf, Hamburg, Germany) was used to remove bubbles trapped in the suspension at 2000 rpm for 5 minutes.

Ink material was 8.0% (w/v) low molecular weight sodium alginate (NaAlg) (Sigma-Aldrich, St. Louis, MO) mixed with 2.0% (w/v) Laponite XLG (BYK Additives Inc., Gonzales, Texas) and 1.0% (w/v) disodium hydrogen phosphate (Na_2HPO_4, Sigma-Aldrich, St. Louis, MO). Herein, Laponite XLG was added to improve the mechanical property of the printed parts and Na_2HPO_4 was to adjust the cross-linking rate of the ink as a cross-linking retardation agent [23]. Specifically, the alginate-based ink was prepared by dispensing the appropriate amount of dry sodium alginate, Laponite XLG, and Na_2HPO_4 powders in DI water at room temperature with continuous mixing. The overhead stirrer was used to ensure thorough hydration of the powders by mixing at 500 rpm for a minimum of 60 minutes. Before printing, the alginate-based ink was degassed using the centrifuge at 2000 rpm for 5 minutes to remove entrapped bubbles.

3.2.2 Printing system and printing protocols

The extrusion system was a micro-dispensing pump machine (nScrypt-3D-450, nScrypt, Orlando, FL). The printing experiments were performed at room temperature. All process parameters have been selected based on a previous study [9]. For alginate-based tympanic membrane patch printing, a 25 gauge (250 μm inner diameter) dispensing tip (EFD Nordson, Vilters, Switzerland) was used to deposit alginate-based structures in the Laponite EP-$CaCl_2$ bath. The printing pressure was 1.38×10^5 Pa (20 psi), the step distances along horizontal and vertical directions were 200 μm, and the printing speed was 2.0 mm/s. After cross-linking in the Laponite EP-$CaCl_2$ bath for 45 minutes,

the tympanic membrane patches were taken out of the bath, and the residual Laponite EP on the surface was rinsed away by pipetting DI water over them.

3.2.3 Mechanical property measurement

To investigate the mechanical properties of the alginate-based materials, tensile test samples with a dogbone-shape were fabricated by casting alginate-based solutions in a customized PDMS mold and cross-linked in $CaCl_2$ baths with different concentrations (0.5%, 1.0%, and 2.0% (w/v)) for 12 hours. Then, uniaxial tensile testing was performed using a mechanical tester (eXpert 4000, Admet, Norwood, MA) at a strain rate of 1.0 mm/min. The stress-strain curves were determined according to the geometry of samples, load and displacement data, and the effective Young's modulus was calculated from the slope of the linear region of the stress-strain curves. It is known that the mechanical properties of the cross-linked alginate samples depend on the concentrations of alginate and $CaCl_2$. To mimic the effective Young's modulus of tympanic membrane, the samples made of 2.0%, 4.0%, 6.0%, and 8.0% (w/v) alginate solutions, which were cross-linked by 0.5%, 1.0%, and 2.0% (w/v) $CaCl_2$, were tested to obtain the optimal combination of alginate and $CaCl_2$. Then, 8.0% (w/v) alginate solutions mixed with 1.0%, 2.0%, 3.0%, and 4.0% (w/v) Laponite XLG were cross-linked by 2.0% (w/v) $CaCl_2$ to investigate the effects of Laponite XLG on the mechanical properties.

3.2.4 Diffusion and gelation time test

To investigate the diffusion and gelation process of the alginate-based solutions, 8.0% (w/v) alginate mixed with 0.5%, 1.0%, and 2.0% (w/v) Na_2HPO_4 were poured in a customized PDMS mold ($20.0 \times 20.0 \times 0.4$ mm^3) and cross-linked in a 2.0% (w/v) $CaCl_2$ bath. The time when the

bottom of the alginate-based sample changed its state to solid was recorded as the diffusion and gelation time.

3.2.5 Statistical analysis

All quantitative values in the text and figures were reported as means ± standard deviation (SD) with n = 3 samples per group. Statistical analysis was performed using analysis of variance (ANOVA) and p-values of less than 0.05 were considered statistically significant.

3.3 Printing Results

3.3.1 Fabrication mechanism of alginate-based tympanic membrane patches

Based on the printing strategy shown in Fig. 1(c), the schematic of the tympanic membrane patch fabrication process is illustrated in Fig. 3. Firstly, alginate-based tympanic membrane patch structures are printed using the alginate-based inks in the Laponite EP-$CaCl_2$ bath as shown in Fig. 3(a). Before cross-linking, sodium alginate chains consist of a family of unbranched binary anionic copolymers of 1,4 linked β-D-mannuronic acid (M units) and α-L-guluronic acid (G units) as shown in the inset of Fig. 3(a). During and after printing, Ca^{2+} ions in the support bath gradually contact and diffuse into the alginate-based structures. When the alginate polymer chains interact with the Ca^{2+} ions, the ionic cross-linking process initiates, and interchain ionic bonds between G blocks are formed with the help of Ca^{2+} ions as shown in Fig. 3(b). After submerging in the Laponite EP-$CaCl_2$ bath, all the G blocks of alginate molecular chains are bonded with each other by Ca^{2+} ions, resulting in a stable calcium alginate network as shown in Fig. 3(c). Thus, the cross-linked alginate-based tympanic membrane patch has enough mechanical strength to be removed from the bath.

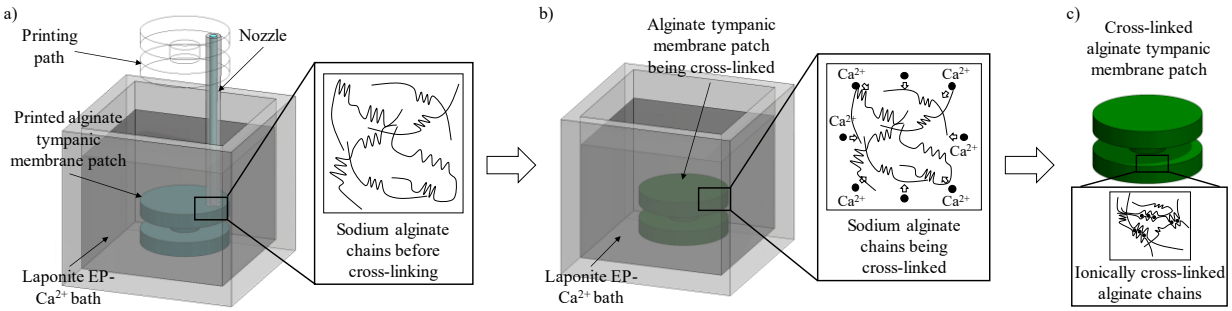

FIGURE 3: Fabrication mechanism of alginate-based tympanic membrane patches. Alginate-based tympanic membrane patch (a) printing and (b) ionic cross-linking in the Laponite EP-$CaCl_2$ bath. (c) Schematic of completely cross-linked alginate-based tympanic membrane patch.

3.3.2 Fabrication results of alginate-based tympanic membrane patches

The alginate-based tympanic membrane patch is designed with a three-layered structure as shown in Fig. 3(c). The diameter and thickness of the top and bottom layers are 5.00 mm and 0.60 mm, respectively. The diameter and thickness of the middle layer are 3.00 mm and 0.80 mm, respectively. The printed alginate-based tympanic membrane patch is illustrated in Fig. 4(a). After keeping in the Laponite EP-$CaCl_2$ bath for 45 minutes, the printed tympanic membrane patches are completely cross-linked and removed from the bath. After rinsing the residual Laponite EP suspension away from each patch surface, the fabricated alginate-based tympanic membrane patches are shown in Fig. 4(b). As seen from Figs. 4(c) and (d), the fabricated structure has a well-defined morphology in both top and side views. Some key dimensions of a randomly selected tympanic membrane patch are measured as follows: the diameter of the top and bottom layers is approximately 5.04 mm, the top/bottom layer thickness is approximately 0.65 mm, and the total thickness is approximately 2.27 mm, which are all close to the designed values of 5.00 mm, 0.60 mm, and 2.00 mm, respectively, indicating the printing accuracy of the proposed nanoclay support bath- enabled printing approach.

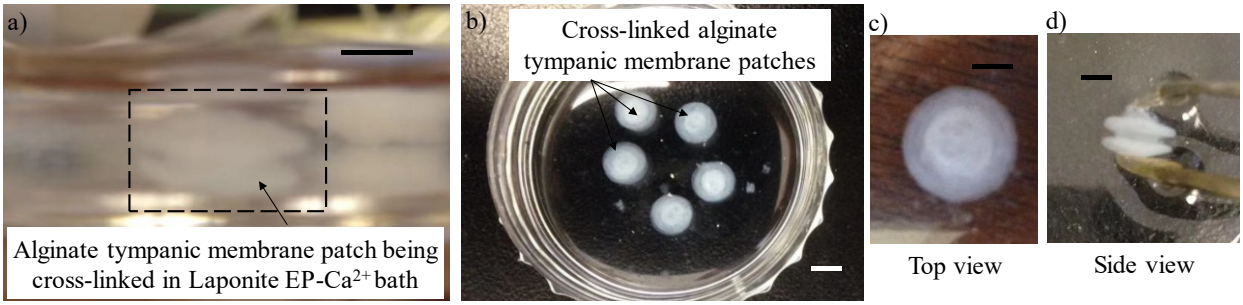

FIGURE 4: Fabrication results of the alginate-based tympanic membrane patches. (a) Alginate-based tympanic membrane patch printing in a Laponite bath. (b) Ionically cross-linked patches. (c) Top view and (d) side view of a representative tympanic membrane patch. Scale bars: 2.0 mm for (a) and 5.0 mm for (b), (c), and (d).

3.4 Discussion

Since the human tympanic membrane has a minimum Young's modulus of approximately 400 kPa in the low stress range (0-1 MPa) [24], it is necessary to design the alginate-based ink to meet the requirement of the mechanical property. The effects of sodium alginate and $CaCl_2$ concentrations on the Young's modulus are measured and shown in Fig. 5(a). It is found that with the increase of alginate and $CaCl_2$ concentrations, the Young's modulus of the alginate-based samples increases, and the 8.0% (w/v) alginate cross-linked by 2.0% (w/v) $CaCl_2$ has the highest Young's modulus (approximately 254 kPa). However, this value is still lower than the required Young's modulus. Thus, Laponite XLG is added into the sodium alginate to enhance the mechanical property of the alginate-based structures. Except being an internal scaffold material, Laponite can be used as a physical cross-linker to improve the mechanical properties of composite hydrogels [12, 23] by physical bonding between Laponite nanosilicates and the alginate molecular network [25]. The effects of Laponite XLG concentration on the Young's modulus are studied, and the results are illustrated in Fig. 5(b). As seen from Fig. 5(b), the addition of Laponite XLG can effectively

increase the Young's modulus, and the alginate sample mixed with 2.0% (w/v) Laponite XLG has the Young's modulus of approximately 450 kPa, which is higher than the minimum requirement.

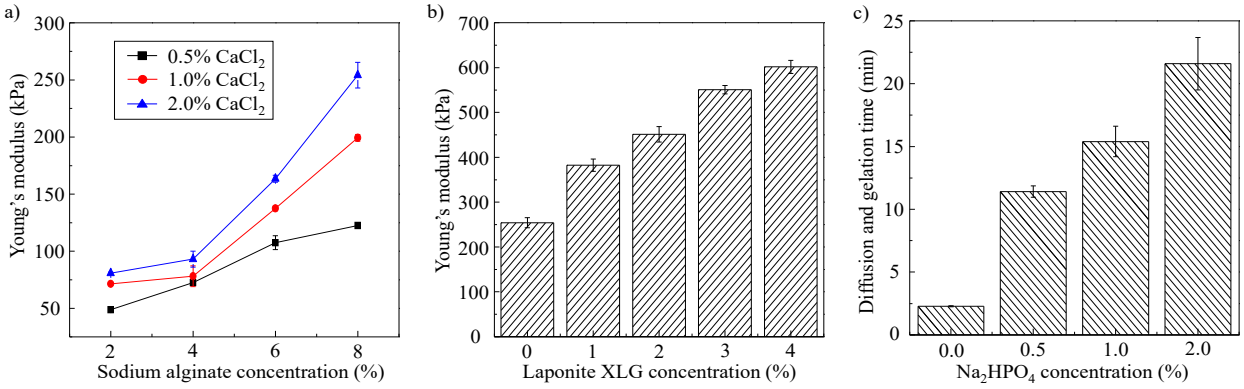

FIGURE 5: Investigations of Young's modulus and diffusion/gelation time of the alginate-based inks. (a) Young's modulus as a function of alginate and $CaCl_2$ concentrations. (b) Young's modulus as a function of Laponite XLG concentration. (c) Diffusion and gelation time as a function of Na_2HPO_4 concentration.

Then, the diffusion and gelation time of the 8.0% (w/v) alginate solutions cross-linked by 2.0% (w/v) $CaCl_2$ is measured as approximately 2.5 minutes. Herein, the gelation time can also be calculated based on the traveling-wave hypothesis and diffusive flux of calcium cations through a gelled structure as $G(t) = \sqrt{2D_c\theta t + L_d^{\,2}} - L_d$, where $G(t)$ is the reaction front position that equals to the sample thickness (0.4 mm) when the sample is completely cross-linked, L_d is the equivalent filter length for the reaction-diffusion model system, which equals to the sample thickness (0.4 mm), D_c is the diffusion coefficient of free calcium cations (for 2.0% (w/v) $CaCl_2$, D_c is 0.77×10^{-9} m^2/s [6]), and θ is a material-related constant, which equals to 0.86 [6]. Thus, the theoretical gelation time (t) is estimated as approximately 6.0 minutes which is close to the measured result. Since the printing of the alginate-based tympanic membrane patches takes around 12.5 minutes,

the gelation rate of the alginate-based inks needs to be adjusted to facilitate the "printing-then-solidification" procedure as proposed in previous studies [9]. When the mixture is exposed to Ca^{2+} ions, the reaction retardation agent Na_2HPO_4 reacts with Ca^{2+} firstly, and then the Ca^{2+} cations are gradually released to react with sodium alginate for cross-linking [23]. By increasing the Na_2HPO_4 concentration, the diffusion and gelation time of the mixed inks increases as shown in Fig. 5(c), and the mixture with 1.0% (w/v) Na_2HPO_4 has a measured diffusion and gelation time (approximately 15 minutes) higher than 12.5 minutes. Thus, the optimal formula of the alginate-based ink is determined as follows: 8.0% (w/v) alginate, 2.0% (w/v) Laponite XLG, and 1.0% (w/v) Na_2HPO_4. The overall fabrication time is around 60 minutes (including 15-minute printing time) in this study, so the nanoclay support bath-enabled printing approach is promising for on-demand fabrication of custom-made artificial tympanic membrane patches for clinical applications.

It is noted that the designed alginate-based tympanic membrane patch has some overhang sections. If the conventional direct ink writing approach is used to print such a patch, supporting structures need to be printed simultaneously, which may complicate the post-treatments and damage the patch when removing the supporting structures. Fortunately, the nanoclay suspension herein provides *in situ* support during printing, resulting in the patches with high shape fidelity as shown in Fig. 4.

4. PRINTING OF PEGDA-BASED NEURAL CHAMBERS IN AIR

4.1 Introduction of Neural Chamber

Neural chambers, one type of microfluidic chambers, have been widely used in organ-on-a-chip devices to incubate neurons and/or other cells and to analyze neuron-to-cell [26-28] or neuron-to-

neuron [29] spread and axonal transport. The typical structure of a neural chamber is illustrated in Fig. 6. Generally, the neural chamber is composed of a neuron compartment and a target compartment connecting by embedded microgrooves. Printing of neural chambers with a similar structure is critical for neuron-related investigations. Due to the excellent cell compatibility and thermal stability of the Laponite XLG-PEGDA nanocomposite hydrogel, it is selected as the build material to print Laponite XLG-PEGDA neural chambers using the nanoclay-enabled direct printing approach.

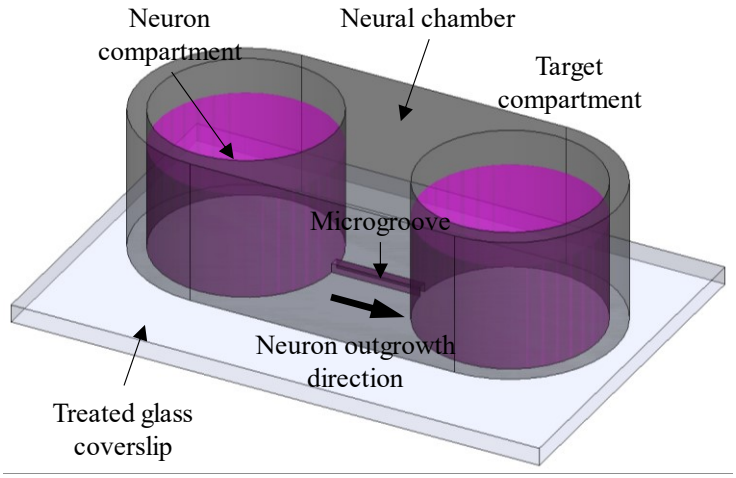

FIGURE 6: Typical neural chamber structure.

4.2 Materials and Methods

4.2.1 Material preparation for PEGDA-based neural chamber printing

For the preparation of the Laponite XLG-PEGDA nanocomposite hydrogel, 10.0% (v/v) PEGDA solution was prepared by mixing stock PEGDA (Mn 700, Sigma-Aldrich, St. Louis, MO) with DI water at room temperature and then dissolving 1.0% (w/v) Irgacure 2959 (I-2959, Ciba, Basel, Switzerland) as a photoinitiator. Laponite XLG powders were added at 6.0% (w/v) into the 10.0% (v/v) PEGDA solution and mixed thorough using the overhead stirrer at 500 rpm for 60 minutes.

The resulted Laponite XLG-PEGDA suspension has the yield-stress property and solid-like behavior during frequency sweeps. The rheological property data can be found in detail in a previous study [12]. It was stored in a sealed container and aged for at least one day. Before each use, the nanocomposite hydrogel suspension was degassed using the centrifuge at 2000 rpm for 5 minutes to remove trapped bubbles. Each neural chamber was printed on a glass cover slip substrate, which was surface modified by forming diethylenetriamine (DETA, United Chemical Technologies Inc., Bristol, PA, T2910KG) self-assembled monolayers via the reaction of the cleaned surface with a 0.1% (v/v) mixture of the organosilane in freshly distilled toluene (Fisher, Pittsburgh, PA, T2904).

4.2.2 Printing system and printing protocols

The trypsin/DETA treatment was firstly performed on the glass cover slips to prepare the receiving substrate for neural chamber printing. Gelatin-methacryloyl (GelMA)-based sacrificial micro-filament arrays were then fabricated on the glass cover slips using a home-made stereolithography (SLA) system. The GelMA-based pre-polymer was prepared by dissolving 10% (w/v) home-made GelMA in warm water (~ 40℃) for around 30 minutes and 0.5% (w/v) lithium phenyl-2,4,6-trimethylbenzoylphosphinate (LAP) as a photo-initiator. The SLA system was developed with a customized DLP (digital light processing)-projector and other required elements such as motorized stages and a UV-transparent pre-polymer vat. The fabricated micro-filaments were controlled at 10 μm in both width and height and 50 μm in spacing between each other. Finally, the neural chambers were printed on the pre-treated and micro-filament-deposited glass cover slips using Laponite XLG-PEGDA. The extrusion system was the micro-dispensing pump machine (nScrypt-3D-450, nScrypt, Orlando, FL), and the printing experiments were performed at room temperature.

All process parameters have been selected based on a previous study [12]. For PEGDA-based neural chamber printing, a 25 gauge (250 μm inner diameter) dispensing tip (EFD Nordson, Vilters, Switzerland) was used to print Laponite XLG-PEGDA nanocomposite hydrogel structures in air. The printing pressure was 1.72×10^5 Pa (25 psi), the step distances along horizontal and vertical directions were 200 μm, and the printing speed was 1.0 mm/s. After printing, the Laponite XLG-PEGDA structures were exposed to UV light (18 W/cm^2, OmniCure Series 2000, wavelength: 320-500 nm, Lumen Dynamics, Mississauga, ON, Canada) for 15 minutes for cross-linking.

4.3 Printing Results

4.3.1 Fabrication mechanism of PEGDA-based neural chambers

Based on the printing strategy shown in Fig. 1(d), the fabrication mechanism is illustrated in Fig. 7. Firstly, Laponite XLG suspension is mixed with PEGDA solution to prepare the nanocomposite hydrogel precursor which is used as the ink material. During mixing, Laponite XLG functions as an internal scaffold material and the nanosilicates interact with ethylene oxide on PEGDA polymer chains through secondary interactions [30, 31] to form physical gels as shown in the inset of Fig. 7(a). This nanocomposite hydrogel precursor has the yield-stress property similar to nanoclay suspensions alone [12] and can be directly printed into 3D structures as shown in Fig. 7(a). After printing, the Laponite XLG-PEGDA chamber is exposed to UV light for chemical cross-linking. Under UV radiation, covalent bonds are formed gradually between PEGDA polymer chains as shown in Fig. 7(b). Finally, stable and irreversible polymer networks are formed by connecting PEGDA chains with covalent bonds, resulting in a completely cross-linked Laponite XLG-PEGDA chamber structure as shown in Fig. 7(c).

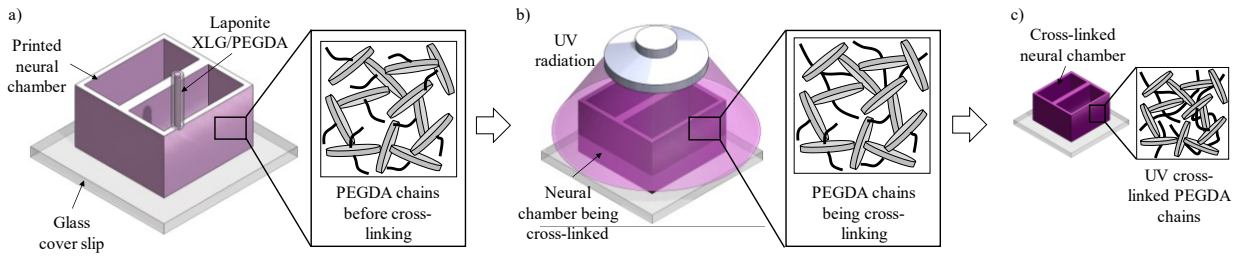

FIGURE 7: Fabrication mechanism of Laponite XLG-PEGDA neural chamber. Laponite XLG-PEGDA neural chamber (a) printing in air and (b) chemical cross-linking under UV radiation. (c) Schematic of completely cross-linked Laponite XLG-PEGDA neural chamber.

4.3.2 Fabrication results of PEGDA-based neural chambers

The designed Laponite XLG-PEGDA neural chamber has a rectangular shape with a length of 20.0 mm, a width of 20.0 mm, and a height of 15.0 mm. To separate the neural chamber into two neuron and target compartments, a 1.0 mm thick middle wall was printed atop the SLA-printed sacrificial micro-filament arrays, which can be removed to form the embedded microgrooves on the glass cover slip. As seen from Fig. 8(a), the yield-stress property of the Laponite XLG-PEGDA nanocomposite hydrogel makes it feasible to directly print Laponite XLG-PEGDA structures in air. As the internal scaffold material, the Laponite XLG suspension helps maintain the shape and integrity of the neural chamber before the liquid PEGDA precursor is cross-linked by UV radiation (Fig. 8(b)). For illustration, the dimensions of a solidified neural chamber are measured as follows: length of 21.2 mm, width of 21.5 mm, height of 14.5 mm, and middle wall thickness of 1.1 mm. Fig. 8(c) shows the two compartments filled with cell medium. Due to the tight adhesion between the neural chamber and the cover slip substrate, the cell medium doesn't leak through the bottom of the fabricated chamber. Since PEGDA precursor of each deposited Laponite XLG-PEGDA filament remains liquid during printing, the adjacent filaments can fuse well with each other. Thus,

the fabricated neural chamber has no gap or interface on each wall, and there is no leakage of cell medium from the chamber.

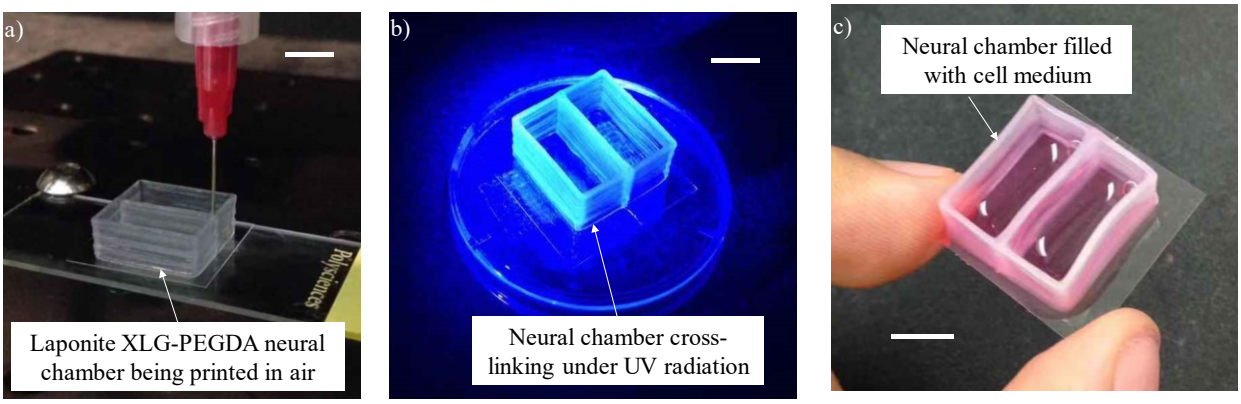

FIGURE 8: Fabrication results of the Laponite XLG-PEGDA neural chamber. Neural chamber (a) printing in air, (b) cross-linking under UV radiation, and (c) filling with cell medium. Scale bars: 10.0 mm.

4.4 Discussion

During nanoclay-enabled direct printing, a self-supporting 3D structure can maintain its shape when the embedded hydrogel precursor is at liquid state as long as the gravity-induced compression stress is lower than the normal yield stress of the Laponite nanoclay suspension. When the compression stress is higher than a critical value, the bottom of printed structure may be liquefied, resulting in the collapse of the whole structure. As a result, it is important to investigate the limitation of the nanoclay-enabled direct printing approach. For a neural chamber having a total height of H and a uniform cross-sectional area of S, the gravitational force on the neural chamber can be calculated as $G = \rho gHS$, where ρ is the density of the nanocomposite ink (1060 kg/m^3), and g is the gravitational acceleration. The gravity-induced compression stress (σ) at the bottom of the chamber is calculated as $\sigma = G/S = \rho gH$. For Laponite XLG-PEGDA structures, the

estimated shear yield stress (τ_{yp}) is 217.5 Pa [12]. According to the octahedral shear stress theory, the normal yield stress (σ_{yp}) can be estimated as 461.4 Pa by using $\sigma_{yp} = \left(3/\sqrt{2}\right)\tau_{yp}$ As a result, the critical height (H_c) of the neural chamber can be estimated as $H_c = \sigma_{yp}/\rho g$ = 44.4 mm. Since the designed neural chamber has a total height of 15.0 mm, which is lower than the critical height, the printed chamber can maintain its shape without collapse.

With the help of the nanoclay suspension, the printed neural chambers remain at liquid state before undergoing photo cross-linking, which enables the adjecent deposited layers to fuse well with each other and effectively prevents the leakage of cell medium from the neural chambers. Since the build material of the neural chambers is the nanoclay Laponite-PEGDA nanocomposite hydrogel, evaporation may be a challenge if the chambers are used in air for a long term. As such, such neural chambers should be utilized for neural cell culturing in a humidity-controllable environment.

5. DISCUSSION ON NANOCLAY YIELD-STRESS SUSPENSION-ENABLED EXTRUSION PRINTING SYSTEM

The nanoclay yield-stress suspension-enabled extrusion printing system has been proved cell friendly in previous studies [9, 12]. The main focus of this paper is to demonstrate the feasibility of using the nanoclay suspension for extrusion bioprinting applications from a manufacturing perspective. While two approaches (nanoclay support bath-enabled printing and nanoclay-enabled direct printing in air) are introduced, they are both enabled by the nanoclay yield-stress suspension. It should be noted that two approaches are completely different: the former uses the low-concentration nanoclay suspension as a support bath while the latter uses the high-concentration

nanoclay suspension as part of build material (bioink). The selection of the most suitable printing approach depends on the geometries of designed parts as well as the properties of build materials.

In support bath-enabled printing, the selection of ink and bath materials must meet the following requirements to facilitate the fabrication process. First, ink material needs to possess a shear elastic modulus that must be at least one order of magnitude higher than that of the support bath material. Otherwise, the shape of the printed filament is easy to be affected by the support bath material [32]. Second, the support bath material must have a suitable yield stress to allow the nozzle to move freely in the bath. Finally, the support bath material should be chemically compatible with the ink material and its cross-linker [33]. The materials selected in the first case perfectly meet aforementioned requirements. Based on the previous rheological measurements [12], the 8.0% (w/v) alginate solution has the elastic modulus higher than that of the nanoclay Laponite EP suspension. In addition, the nanoclay Laponite EP suspension has the yield stress of ~ 10 Pa, falling in the yield-stress range (1-400 Pa) of the commonly used support bath materials [7, 9]. Moreover, different from other support bath materials such as Carbopol [7], nanoclay Laponite EP has excellent compatibility with $CaCl_2$ and does not have any chemical reaction with alginate, making it one of the best support baths for alginate printing. Therefore, nanoclay Laponite EP-$CaCl_2$ and alginate-based ink have been selected as the exemplary bath and ink materials for the nanoclay support bath-enabled printing. However, some constraints should be noted regarding this approach. First, the applied cross-linking mechanism should not disturb the “house-of-card” arrangement of the nanoclay support bath. Second, printed 3D structures should have sufficient mechanical strength to be removed from the nanoclay support bath. For some hydrogels with weak mechanical

properties such as collagen, it may not be suitable to use the nanoclay support bath-enabled printing approach.

For the nanoclay-enabled direct printing approach, the main requirement of ink materials is that hydrogel precursors cannot have chemical reactions with the nanoclay suspension which may cause the nanocomposite hydrogels to lose the self-supporting capacity. It has been proved that nanoclay is compatible with various hydrogels such as alginate [15], gelatin [16], and Pluronic F127 [34], to name a few. All these materials are potentially able to be printed into 3D structures via the nanoclay-enabled direct printing approach. Furthermore, the maximum height of a printed structure is limited by the yield stress of the nanocomposite hydrogel being selected. For the neural chamber printing case, the chamber has the maximum height of ~ 15 mm. Thus, the nanoclay Laponite-PEGDA ink with the yield shear stress of ~ 200 Pa has been selected. If the required height increases, the concentration of nanoclay Laponite should be increased accordingly to improve the self-supporting capacity. In addition, it should be pointed out that the addition of nanoclay Laponite should not alter the overall material properties of bioinks in order to apply this printing approach.

6. CONCLUSIONS AND FUTURE WORK

The effectiveness of the nanoclay suspension enabled extrusion-based 3D printing system has been presented, in which Laponite nanoclay suspensions with yield-stress property are utilized to facilitate the printing of 3D soft structures from different biocompatible ink materials. Specifically, two different printing strategies have been demonstrated. Firstly, the Laponite EP nanoclay suspension is used as a yield-stress support bath material, and alginate-based tympanic membrane

patches are fabricated using the nanoclay support bath-enabled 3D printing approach. Secondly, the Laponite XLG nanoclay suspension is utilized as a yield-stress internal scaffold material for direct printing in air, and Laponite XLG-PEGDA based neural chambers with self-supporting property are printed. Due to the excellent cell compatibility of both Laponite EP [9] and XLG [12], the proposed nanoclay suspension-based 3D printing system presents great potential for cell printing/culturing applications in the future.

It is noted that while alginate and PEGDA are utilized in this study, the 3D printing system also provides versatile approaches for effective extrusion 3D printing of other ink materials, which may require special accommodation of their cross-linking rate. For future work, living cells can be mixed with the alginate-based ink to print cell-laden tympanic membrane patches, which can be used to support in-growth of surrounding native tympanic membrane. The animal studies of tympanic membrane repair should be performed to verify the functional effectiveness of the printed alginate-based tympanic membrane patches. For neural chamber applications, neural cells will be incubated in the printed PEGDA-based neural chambers to test the function of the chambers and investigate the resulting axon outgrowth. In addition, such a printing system can be extended to the printing of hydrophobic inks by using applicable nanoclay yield-stress suspensions such as a fumed silica suspension. For broad applications of the presented printing technology, the microstructure and transition mechanism between the jamming and unjamming state of the nanoclay suspension should be further explored interdisciplinarily.

ACKNOWLEDGEMENTS

This research was partially supported by NSF (CMMI-1762941), and the assistance from A. Compaan is highly appreciated.

REFERENCES

[1] Murphy, S. V., and Atala, A., 2014, "3D bioprinting of tissues and organs," *Nature Biotechnology*, 32(8), p. 773.

[2] Mandrycky, C., Wang, Z., Kim, K., and Kim, D. H., 2016, "3D bioprinting for engineering complex tissues," *Biotechnology Advances*, 34(4), pp. 422-434.

[3] Ozbolat, I. T., Peng, W., and Ozbolat, V., 2016, "Application areas of 3D bioprinting," *Drug Discovery Today*, 21(8), pp. 1257-1271.

[4] Phillippi, J. A., Miller, E., Weiss, L., Huard, J., Waggoner, A., and Campbell, P., 2008, "Microenvironments engineered by inkjet bioprinting spatially direct adult stem cells toward muscle‐and bone‐like subpopulations," *Stem Cells*, 26(1), pp. 127-134.

[5] Kucukgul, C., Ozler, S. B., Inci, I., Karakas, E., Irmak, S., Gozuacik, D., and Koc, B., 2015, "3D bioprinting of biomimetic aortic vascular constructs with self-supporting cells," *Biotechnology and Bioengineering*, 112(4), pp. 811-821.

[6] Xiong, R., Zhang, Z., Chai, W., Huang, Y., and Chrisey, D. B., 2015, "Freeform drop-on-demand laser printing of 3D alginate and cellular constructs," *Biofabrication*, 7(4), p. 045011.

[7] Jin, Y., Compaan, A., Bhattacharjee, T., and Huang, Y., 2016, "Granular gel support-enabled extrusion of three-dimensional alginate and cellular structures," *Biofabrication*, 8(2), p. 025016.

[8] Ahlfeld, T., Cidonio, G., Kilian, D., Duin, S., Akkineni, A. R., Dawson, J. I., and Gelinsky, M., 2017, "Development of a clay based bioink for 3D cell printing for skeletal application," *Biofabrication*, 9(3), p. 034103.

[9] Jin, Y., Compaan, A., Chai, W., and Huang, Y., 2017, "Functional nanoclay suspension for printing-then-solidification of liquid materials," *ACS Applied Materials and Interfaces*, 9(23), pp. 20057-20066.

[10] Hockaday, L. A., Kang, K. H., Colangelo, N. W., Cheung, P. Y. C., Duan, B., Malone, E., and Chu, C. C., 2012, "Rapid 3D printing of anatomically accurate and mechanically heterogeneous aortic valve hydrogel scaffolds*," Biofabrication*, 4(3), p. 035005.

[11] Schacht, K., Jüngst, T., Schweinlin, M., Ewald, A., Groll, J., and Scheibel, T., 2015, "Biofabrication of cell-loaded 3D spider silk constructs," *Angewandte Chemie International Edition*, 54(9), pp. 2816-2820.

[12] Jin, Y., Liu, C., Chai, W., Compaan, A., and Huang, Y., 2017, "Self-supporting nanoclay as internal scaffold material for direct printing of soft hydrogel composite structures in air," *ACS Applied Materials and Interfaces*, 9(20), pp. 17456-17465.

[13] Zhang, Z. F., Ma, X., Wang, H., and Ye, F., 2018, "Influence of polymerization conditions on the refractive index of poly (ethylene glycol) diacrylate (PEGDA) hydrogels," Applied Physics A, 124(4), p. 283.

[14] Chang, C. W., van Spreeuwel, A., Zhang, C., and Varghese, S., 2010, "PEG/clay nanocomposite hydrogel: a mechanically robust tissue engineering scaffold," *Soft Matter*, 6(20), pp. 5157-5164.

[15] Ghadiri, M., Chrzanowski, W., Lee, W. H., Fathi, A., Dehghani, F., and Rohanizadeh, R., 2013, "Physico-chemical, mechanical and cytotoxicity characterizations of Laponite®/alginate nanocomposite," *Applied Clay Science*, 85, pp. 64-73.

[16] Gaharwar, A. K., Avery, R. K., Assmann, A., Paul, A., McKinley, G. H., Khademhosseini, A., and Olsen, B. D., 2014, "Shear-thinning nanocomposite hydrogels for the treatment of hemorrhage," *ACS Nano*, 8(10), pp. 9833-9842.

[17] Strens, D., Knerer, G., Van Vlaenderen, I., and Dhooge, I. J. M., 2012, "A pilot cost-of-illness study on long-term complications/sequelae of AOM," *B-ENT*, 8(3), p. 153.

[18] Kozin, E. D., Black, N. L., Cheng, J. T., Cotler, M. J., McKenna, M. J., Lee, D. J., and Remenschneider, A. K., 2016, "Design, fabrication, and in vitro testing of novel three-dimensionally printed tympanic membrane grafts," *Hearing research*, 340, pp. 191-203.

[19] Luginbuehl, V., Wenk, E., Koch, A., Gander, B., Merkle, H.P., and Meinel, L., 2005, "Insulin-like growth factor I-releasing alginate-tricalciumphosphate composites for bone regeneration," *Pharmaceutical Research*, 22(6), pp. 940-950.

[20] Hott, M. E., Megerian, C. A., Beane, R., and Bonassar, L. J., 2004, "Fabrication of tissue engineered tympanic membrane patches using computer-aided design and injection molding," *The Laryngoscope*, 114(7), pp. 1290-1295.

[21] Weber, D. E., Semaan, M. T., Wasman, J. K., Beane, R., Bonassar, L. J., and Megerian, C. A., 2006, "Tissue-engineered calcium alginate patches in the repair of chronic chinchilla tympanic membrane perforations," *The Laryngoscope*, 116(5), pp. 700-704.

[22] Hong, P., Bance, M., and Gratzer, P. F., 2013, "Repair of tympanic membrane perforation using novel adjuvant therapies: a contemporary review of experimental and tissue engineering studies," *International Journal of Pediatric Otorhinolaryngology*, 77(1), pp. 3-12.

[23] Jin, Y., Chai, W., and Huang, Y., 2018, "Fabrication of stand-alone cell-laden collagen vascular network scaffolds using fugitive pattern-based printing-then-casting approach," *ACS Applied Materials and Interfaces*, 10(34), pp. 28361-28371.

[24] Cheng, T., Dai, C., and Gan, R. Z., 2007, "Viscoelastic properties of human tympanic membrane," *Annals of Biomedical Engineering*, 35(2), pp. 305-314.

[25] Loizou, E., Butler, P., Porcar, L., Kesselman, E., Talmon, Y., Dundigalla, A., and Schmidt, G., 2005, "Large scale structures in nanocomposite hydrogels," *Macromolecules*, 38(6), pp. 2047-2049.

[26] Bauer, D., Alt, M., Dirks, M., Buch, A., Heilingloh, C. S., Dittmer, U., and Eis-Hübinger, A. M., 2017, "A therapeutic antiviral antibody inhibits the anterograde directed neuron-to-cell spread of herpes simplex virus and protects against ocular disease," *Frontiers in Microbiology*, 8, p. 2115.

[27] Johnson, B. N., Lancaster, K. Z., Hogue, I. B., Meng, F., Kong, Y. L., Enquist, L. W., and McAlpine, M. C., 2016, "3D printed nervous system on a chip," *Lab on a Chip*, 16(8), pp. 1393-1400.

[28] Santhanam, N., Kumanchik, L., Guo, X., Sommerhage, F., Cai, Y., Jackson, M., Martin, C., Saad, G., McAleer, C. W., Wang, Y., Lavado, A., Long, C. J., Hickman, J. J., 2018, "Stem cell derived phenotypic human neuromuscular junction model for dose response evaluation of therapeutics," *Biomaterials*, 166, pp. 64-78.

[29] Freundt, E. C., Maynard, N., Clancy, E. K., Roy, S., Bousset, L., Sourigues, Y., and Brahic, M., 2012, "Neuron-to-neuron transmission of α-synuclein fibrils through axonal transport," *Annals of Neurology*, 72(4), pp. 517-524.

[30] Baghdadi, H. A., Sardinha, H., and Bhatia, S. R., 2005, "Rheology and gelation kinetics in laponite dispersions containing poly (ethylene oxide)," *Journal of Polymer Science Part B: Polymer Physics*, 43(2), pp. 233-240.

[31] Chang, C. W., van Spreeuwel, A., Zhang, C., and Varghese, S., 2010, "PEG/clay nanocomposite hydrogel: a mechanically robust tissue engineering scaffold," *Soft Matter*, 6(20), pp. 5157-5164.

[32] Jin, Y., Chai, W., and Huang, Y., 2017, "Printability study of hydrogel solution extrusion in nanoclay yield-stress bath during printing-then-gelation biofabrication," *Materials Science and Engineering: C*, 80, pp. 313-325.

[33] Muth, J. T., Vogt, D. M., Truby, R. L., Mengüç, Y., Kolesky, D. B., Wood, R. J., and Lewis, J. A., 2014, "Embedded 3D printing of strain sensors within highly stretchable elastomers," *Advanced Materials*, 26(36), pp. 6307-6312.

[34] Wu, C. J., Gaharwar, A. K., Chan, B. K., and Schmidt, G., 2011, "Mechanically tough pluronic F127/laponite nanocomposite hydrogels from covalently and physically cross-linked networks," *Macromolecules*, 44(20), pp. 8215-8224.